European Journal of Pharmaceutics and Biopharmaceutics 75 (2010) 354–365

Contents lists available at ScienceDirect

European Journal of Pharmaceutics and Biopharmaceutics

journal homepage: www.elsevier.com/locate/ejpb

Research paper

Combined use of ordered mesoporous silica and precipitation inhibitors for improved oral absorption of the poorly soluble weak base itraconazole

Michiel Van Speybroeck [a], Raf Mols [a], Randy Mellaerts [b], Thao Do Thi [a], Johan A. Martens [b], Jan Van Humbeeck [c], Pieter Annaert [a], Guy Van den Mooter [a], Patrick Augustijns [a,*]

[a] Laboratory for Pharmacotechnology and Biopharmacy, Katholieke Universiteit Leuven, Leuven, Belgium
[b] Centre for Surface Chemistry and Catalysis, Katholieke Universiteit Leuven, Heverlee, Belgium
[c] Department of Metallurgy and Materials Engineering, Katholieke Universiteit Leuven, Heverlee, Belgium

ARTICLE INFO

Article history:
Received 13 January 2010
Accepted in revised form 19 April 2010
Available online 24 April 2010

Keywords:
Mesoporous silica
SBA-15
Itraconazole
Supersaturation
Precipitation inhibitors
Bioavailability

ABSTRACT

The release of poorly soluble drugs from mesoporous silicates is often associated with the generation of supersaturation, which implies the risk of drug precipitation and reduced availability for absorption. The aim of this study was to enhance the *in vivo* performance of an ordered mesoporous silicate (SBA-15) by combining it with the precipitation inhibitors hydroxypropylmethylcellulose (HPMC) and hydroxypropylmethylcellulose acetate succinate (HPMCAS). The poorly soluble weak base itraconazole was used as a model compound. Formulations were prepared by physically blending itraconazole-loaded SBA-15 with the precipitation inhibitors. *In vitro* release experiments implementing a transfer from simulated gastric fluid to simulated intestinal fluid were used to evaluate the pharmaceutical performance. Subsequently, the formulations were evaluated *in vivo* in rats. When high enough amounts of HPMC were co-administered with itraconazole-loaded SBA-15 (itraconazole:SBA-15:HPMC 1:4:6), the extent of absorption was increased by more than 60% when compared to SBA-15 without precipitation inhibitors (AUC 14,937 ± 1617 versus 8987 ± 2726 nM h). HPMCAS was found ineffective in enhancing the *in vivo* performance of SBA-15 due to its insolubility in the stomach. The results of this study demonstrate that the pharmaceutical performance of SBA-15 is enhanced through addition of an appropriate precipitation inhibitor.

1. Introduction

Contemporary approaches to drug discovery often lead to the identification of drugs with high lipophilicity and low aqueous solubility [1–3]. The concomitant low and variable oral absorption of poorly soluble drugs constitutes one of the most important challenges to modern drug development. A widely investigated approach to circumvent solubility/dissolution-limited bioavailability is the use of amorphous drug forms. The high internal energy of the amorphous state relative to the crystalline state underlies an increased solubility and dissolution rate and can thus enhance bioavailability [4]. However, the amorphous state also holds the risk of converting back to the energetically more favorable crystalline state during processing or storage. In order to enhance physical stability, amorphous drugs are usually formulated as dispersions in a physiologically inert carrier matrix [5,6]. Although this approach, the so-called solid dispersion approach, has enjoyed widespread interest from formulation scientists, the number of commercialized solid dispersions remains very limited. In addition to issues related to the method of preparation and dosage form development, metastability constitutes a major drawback of the solid dispersion approach [7].

A technology that is gaining momentum as a means to stabilize amorphous drugs is adsorption in/on mesoporous materials. The term *mesoporous* designates porous materials that exhibit pores with diameters between 2 and 50 nm (IUPAC definition). Although a variety of chemically different mesoporous materials have been described, silica-based materials have been most widely investigated in the context of drug delivery. The mechanism by which mesoporous silicates stabilize amorphous drugs is related to so-called *finite-size effects*; when confined in a pore with a size of only a few molecular diameters, the properties of a solid are greatly altered [8]. Since the long-range ordering associated with crystallization cannot extend beyond the pore diameter, crystallization is greatly hindered and essentially suppressed. Although most of the knowledge on confined systems has been obtained from studies using small, non-therapeutic, organic molecules such as cyclohexane [9], benzene [9], toluene [10], or methanol [11], a continuously increasing number of papers addresses the confinement of drug molecules. Various studies have demonstrated that constraining a drug to the pores of a mesoporous silicate leads to

* Corresponding author at: Laboratory for Pharmacotechnology and Biopharmacy, Katholieke Universiteit Leuven, Belgium Building O&N2, Herestraat 49-box 921, BE-3000 Leuven, Belgium. Tel.: + 32 16 330301; fax: +32 16 330305.
E-mail address: Patrick.augustijns@pharm.kuleuven.be (P. Augustijns).

0939-6411/$ - see front matter © 2010 Elsevier B.V. All rights reserved.
doi:10.1016/j.ejpb.2010.04.009

amorphization. Furthermore, these mesoporous silica-based formulations show excellent physical stability, even under conditions of elevated temperature/relative humidity [12–14].

Upon contact with water, the confined amorphous material dissolves and diffuses out of the pores. Current knowledge suggests that the most important factors affecting drug release from mesoporous silicates are the pore diameter and the particle size/morphology [15–18]. It is noteworthy that this may not be true for surface-functionalized mesoporous silicates, which are not under consideration here. Depending on the pore diameter and the particle size/morphology, release of the confined drug may occur in the order of minutes, hours, or even days. *Ordered* mesoporous silicates, such as SBA-15 [19], MCM-41 [20], or FSM-16 [21], offer the advantage that their pore diameter can be adjusted through modification of the material synthesis, which enables the formulation scientist to gain control over the drug release rate.

Although numerous studies have demonstrated enhanced *in vitro* dissolution properties for a wide variety of compounds using mesoporous silicates, the number of *in vivo* studies remains very limited [22]. The putative mechanism by which mesoporous silicates improve drug absorption is by creating drug supersaturation *in vivo* [23]. By virtue of Fick's first law, increased intraluminal concentrations may enhance the flux of drug across the gastrointestinal epithelium and thus increase absorption. However, simply releasing the drug in its supersaturated state in the gastrointestinal tract may not be sufficient for optimal *in vivo* performance, as rapid precipitation to an energetically more favorable but less soluble form may jeopardize absorption [24–27]. The *in vivo* performance of mesoporous silicates might therefore be enhanced through the addition of an excipient that retards or prevents precipitation of the released fraction. This type of approach, i.e., whereby a formulation component that generates supersaturation (a *spring*) is combined with a precipitation inhibitor (a *parachute*), has earlier been referred to as the *spring-and-parachute* approach [24]. Various dissolution-enhancing technologies that are associated with the generation of supersaturation, e.g., the use of high solubility salts [24] or lipid-based systems [25,27], have been shown to benefit from the incorporation of a precipitation inhibitor. Although it may be assumed that the *in vivo* performance of mesoporous silicates is enhanced through the addition of a precipitation inhibitor, this has not yet been assessed.

The aim of the present study was therefore to evaluate the *in vivo* performance of formulations consisting of a drug-loaded mesoporous silicate and a precipitation inhibitor. For various reasons, we selected SBA-15 as mesoporous silicate. First, SBA-15 can be regarded as one of the most regular mesoporous materials currently available. It features a system of uniform, parallel, cylindrical mesopores that are arranged in a honeycomb-like lattice and a complementary system of disordered micropores [19]. Second, SBA-15 can be synthesized over a broad range of pore diameters going from 5 to 30 nm with a very narrow pore size distribution. Third, SBA-15 exhibits a high internal pore volume, which enables drug loadings as high as 50% (w/w) [13,28]. All of these features render SBA-15 probably the most interesting mesoporous silicate toward immediate release applications. As a model compound, we selected the triazole antifungal agent itraconazole (ITZ) (Fig. 1). ITZ can be categorized as a Biopharmaceutical Classification System Class II drug [29], i.e., it permeates well across the gastrointestinal epithelium [30], but poor solubility limits its absorption. Due to its extremely low aqueous solubility (Table 1), ITZ plasma exposure is subject to significant inter- and intrasubject variability [31–33]. ITZ is weakly basic in nature and possesses two nitrogen atoms (p*Ka* 2 and 3.7) that can be protonated in the physiological range, resulting in a pronounced pH-dependent solubility (Table 1) [30]. Earlier work has demonstrated that ITZ bioavailability is increased upon co-administration of acidic beverages such as cola [34,35] and decreased in conditions of elevated gastric pH [36]. ITZ for oral administration is commercialized under the trade name Sporanox®, which is a capsule-based formulation containing beads coated with an ITZ solid dispersion in hydroxypropylmethylcellulose (HPMC) (ITZ:HPMC ratio 1:1.5). The precipitation inhibitors used within this study were HPMC and hydroxypropylmethylcellulose acetate succinate (HPMCAS). The selection of these polymers was based on the results of a prior supersaturation screening conducted in our laboratory, demonstrating that, out of a wide variety of excipients, only HPMC and HPMCAS were capable of providing significant ITZ supersaturation stabilization. Formulations were prepared by physically blending ITZ-loaded SBA-15 with the precipitation inhibitors. The pharmaceutical performance of these formulations was assessed by means of *in vitro* release experiments implementing a transfer of simulated gastric fluid to simulated intestinal fluid. Subsequently, the formulations were tested *in vivo* in rats. The performance of the SBA-15-based formulations was benchmarked against that of crystalline ITZ and Sporanox®.

2. Materials and methods

2.1. SBA-15 synthesis

SBA-15 was synthesized as described by Galarneau et al. [37]. Twelve grams of Pluronic P123 (BASF, Antwerp, Belgium) was dissolved in a mixture of 60 g deionized water (17.8 MΩ) and 120 g of 2 M HCl (Fischer Scientific, Leicestershire, UK). Water was purified

Table 1
Physicochemical properties of ITZ [30].

Molecular weight	705.6 g/mol
cLog P	6.2
p*Ka*	2 and 3.7
Melting point	165–169 °C
Solubility in water (pH 7)	~1 ng/ml
Solubility in 0.1 N HCl (pH 1)	~5 μg/ml

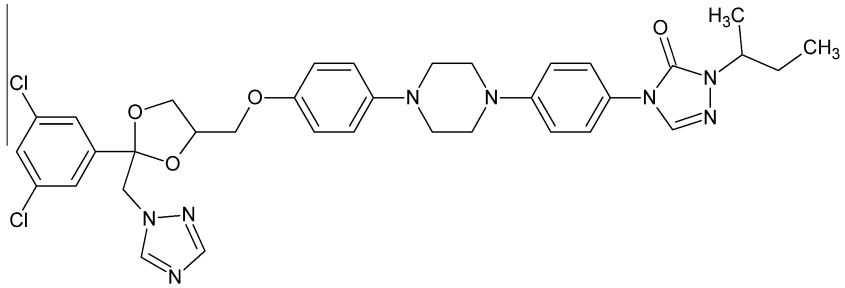

Fig. 1. Structural formula of ITZ.

using an Elga Maxima system (Elga Ltd., High Wycombe Bucks, UK). This mixture was stirred overnight, to ensure complete dissolution of Pluronic P123. Subsequently, 25.26 g of tetraethylorthosilicate (Acros Organics, Geel, Belgium) was added to the acidic Pluronic P123 solution under magnetic stirring, while a temperature of 35 °C was maintained. Stirring was continued for another 5 min before switching to quiescent synthesis conditions at 35 °C for 24 h. In a next step (ripening), the reaction vessel was put in an oven at 90 °C and kept isothermally for another 48 h. After cooling to room temperature, the obtained suspension was vacuum filtered over a 0.45-μm membrane filter (Millipore, Brussels, Belgium), rinsed with 200 ml of deionized water, and dried at 40 °C under reduced pressure (10^{-3} bar) for 12 h. Finally, the SBA-15 powder was calcined at 550 °C for 8 h to remove the Pluronic P123 from the pores.

2.2. Nitrogen adsorption and calculations

Nitrogen adsorption–desorption isotherms of the SBA-15 powder were recorded at −196 °C using a Micromeritics Tristar 3000-apparatus (Norcross, GA). All samples were pre-treated at 300 °C for 12 h under nitrogen flushing prior to analysis. The total surface area was calculated using the Brunauer–Emmett–Teller equation in the relative pressure range between 0.05 and 0.2 [38]. The total and micropore volume were estimated using the *t*-plot method [39]. The pore size distribution was derived from the adsorption branches of the nitrogen isotherms using the Barrett–Joyner–Halenda method [40].

2.3. ITZ loading procedure

ITZ (kindly donated by Janssen Pharmaceutica, Beerse, Belgium) was loaded into SBA-15 by impregnating the SBA-15 powder with a concentrated solution of ITZ in methylene chloride (Fischer Scientific) (50 mg/ml) to obtain a drug loading of 1:4 and 1:1.5 (w:w). The moist powder thus obtained was stirred with a spatula until seemingly dry, after which it was dried further at 40 °C under reduced pressure (10^{-3} bar) for 48 h to remove any residual methylene chloride from the pores. Note that prior head-space chromatography experiments had indicated that the residual concentration of methylene chloride in ITZ-loaded SBA-15 is below the FDA limit of 600 ppm (unpublished results).

2.4. ITZ content quantification

The drug content of the ITZ-SBA-15 formulations was determined by suspending 5 mg of the formulation in 10 ml of methanol (Fisher Scientific) ($n = 3$). These suspensions were first sonicated for 30 min (Branson 3510, 40 kHz, Branson Ultrasonics, Danbury, CT) and subsequently put in a rotary mixer (Snijders, Tilburg, The Netherlands) for 24 h, after which the SBA-15 was separated from the ITZ solution by filtration (PTFE-membrane filter, 0.45 μm pore size) (Macherey–Nagel, Düren, Germany). The concentration of the drug in solution was determined by UV-spectrometry, using a Tecan Infinite M200 plate reader (Tecan Benelux, Mechelen, Belgium) and flat bottom, transparent 96-well plates (UV-star) (Greiner Bio-One, Frickenhausen, Germany). The wavelength used for quantification was 260 nm. The ITZ concentrations were calculated using Lambert–Beer's law, by interpolation from a calibration curve. A linear response was obtained for concentrations ranging from 5 to 100 μg/ml.

2.5. Preparation of glassy ITZ

Glassy ITZ was prepared as described by Janssens et al. [41].

2.6. Differential scanning calorimetry (DSC)

DSC experiments were performed on a TA Instruments Q-2000 apparatus (TA Instruments, Leatherhead, UK) at a heating rate of 20 °C/min. Scans were recorded between 0 and 200 °C. Dry nitrogen was used as the purge gas through the DSC cell (flow rate of 50 ml/min). All experiments were carried out in open, crimped aluminum pans (TA Instruments). The sample size varied between 5 and 8 mg. Under these experimental conditions, crystalline ITZ in a 0.5% (w:w%) ITZ:SBA-15 physical mixture could still be detected. All thermograms were recorded in duplicate, and all data handling was performed using the Universal Analysis 2000 software package (TA Instruments).

2.7. Preparation of SGF and FaSSIF

Simulated gastric fluid (SGF) (pH 1.2) was prepared by adding 0.2% (w/v) NaCl (Fisher Scientific) to 0.1 M HCl (Fisher Scientific). Fasted state simulated intestinal fluid (FaSSIF) (pH 6.5) was prepared according to the formula described by Vertzoni et al. [42]. The following chemicals were used for the preparation of FaSSIF: sodium taurocholate (practical grade) (ICN Biomedicals, Eschwege, Germany), lecithin (Phospholipon 90G, Nattermann Phospholipid, Köln, Germany), $NaH_2PO_4{\cdot}H_2O$ (Fisher Scientific), and chloroform (Chemlab, Zedelgem, Belgium).

2.8. In vitro supersaturation assay

A cosolvent quench-based approach was used to generate ITZ supersaturation. The media of interest were spiked with an ITZ stock solution (10 mg/ml) in dimethylsulfoxide (DMSO) (Acros Organics), to induce an initial degree of supersaturation (DS) of 10 and 20. The DS is defined as the ratio of the concentration in solution over the thermodynamic solubility. For example: the equilibrium solubility of ITZ in FaSSIF was determined to be 0.3 μg/ml, so FaSSIF was spiked to obtain a (theoretical) initial concentration of 3 μg/ml (DS 10) and 6 μg/ml (DS 20). A similar approach was used for SGF. The final DMSO concentration thus obtained never exceeded 2% (v/v). ITZ supersaturation was evaluated in SGF and FaSSIF, in the presence or absence of 0.05% (w/v) excipient. The excipients used for stabilization of supersaturation were HPMC (grade E5) (Dow, Midland, MI) and HPMCAS (grade LF) (Shin-Etsu, Tokyo, Japan). Because prior work [53] had suggested that SBA-15 had a negative effect on ITZ supersaturation in SGF, we also evaluated the stability of ITZ precipitation when SBA-15 was predispersed in SGF (0.05% w/v).

The setup used consisted of a water bath, placed on multiple-position magnetic stirring plate (IKAmag RO 10 power, IKA Werke, Staufen, Germany). Glass vials containing 40 ml of medium were fixated in the water bath, while the temperature was maintained at 37 °C. Agitation was accomplished through magnetic stirring (cross-shaped magnetic stirrings discs, 10 mm diameter, VWR International, Brussels, Belgium), at a stirring speed of 5 on the nominal scale of the stirrer (ca 480 rpm). Following generation of supersaturation, 1-ml samples were withdrawn at 10, 30, 60, and 120 min (and for the FaSSIF samples additionally at 240 min) and filtered over a 0.45-μm PTFE filter (Macherey–Nagel). All filters were pre-rinsed with 10 ml of a saturated solution of ITZ in the medium under investigation, in order to prevent adsorption to the filter. All samples were diluted appropriately in mobile phase prior to analysis. The samples in SGF were quantified by UV-spectrometry as described in Section 2.4. Quantification of the FaSSIF samples was performed by HPLC-UV (see 2.13).

2.9. Solubility assay

ITZ equilibrium solubilities were determined in all the media that were used for the supersaturation experiments, i.e., in SGF and FaSSIF with or without 0.05% (w/v) of excipient. The influence of DMSO, originating from the solvent-induced supersaturation, on the equilibrium solubility was also assessed; at the concentrations tested (maximum 2% v/v), DMSO did not affect the thermodynamic solubility of ITZ. Solubilities were determined using a shake-flask method: approximately 2 mg of ITZ was dispersed in 1.5 ml of medium, shaken for 48 h at 37 °C, and filtered over a 0.45-μm PTFE filter (Macherey–Nagel). The filtrate was diluted appropriately in mobile phase and analyzed by HPLC-UV (see Section 2.13).

2.10. Preparation of ITZ:SBA-15:precipitation inhibitor formulations

The ITZ:SBA-15:precipitation inhibitor formulations formulations were prepared by physically blending ITZ:SBA-15 1:4 with either HPMC or HPMCAS. Two weight ratio's of ITZ:precipitation inhibitor were used: 1:1.5 and 1:6. The weight ratio of 1:1.5 was used to allow for an appropriate comparison with Sporanox®, which also has an ITZ:HPMC ratio of 1:1.5. Since we assumed that the faster drug release from SBA-15 would require higher amounts of stabilizer in order to effectively inhibit precipitation, we also applied an ITZ:precipitation inhibitor ratio of 1:6.

2.11. In vitro release in SGF

Experiments in SGF were conducted under sink and supersaturating conditions. For the sink-type experiments, 1% (w/v) of sodium lauryl sulfate (SLS) (Merck Schuchardt, Hohenbrunn, Germany) was added. This medium assured the maintenance of sink conditions throughout the experiment (solubility of ITZ in SGF + 1% SLS was determined to be 750 μg/ml). Prewarmed medium (40 ml, 37 °C) was added to glass vials containing 4 ± 0.1 mg of ITZ (as formulation or as crystalline drug). Subsequently, the vials were put in a rotary mixer (Snijders) that was positioned in an oven (37 °C). The stirring intensity of the rotary mixer was set at 1 of the nominal scale of the device. At 5, 10, 30, 60, and 120 min, 1-ml samples were withdrawn and filtered over a 0.45-μm PTFE filter (Macherey–Nagel). All samples were quantified without further dilution using UV-spectrometry, as described in Section 2.4.

2.12. In vitro release with pH-shift

In order to simulate the *in vivo* situation, *in vitro* release experiments implementing a transfer of SGF to FaSSIF were also conducted. The experiments were carried out in a similar fashion as described in the previous paragraph, with some modifications. Eight milligrams of ITZ (as crystalline powder or as formulation) were weighed out in a vial and 40 ml of prewarmed (37 °C) SGF (without SLS) was added. After 60 min, 4 ml of the SGF medium was transferred to 36 ml of FaSSIF. The transfer was thus accompanied with a 10-fold dilution. The relative amount in solution in FaSSIF after transfer from SGF was calculated based on the initial amount of ITZ present in FaSSIF (i.e., 10% of the ITZ dose that was dispersed in the SGF-phase). The formula of FaSSIF for the pH-shift experiments was adapted such that the addition of 10% of SGF resulted in similar lecithin and taurocholate concentrations and the same pH as *real* FaSSIF. The formula for this modified FaSSIF was as follows: 3.33 mM sodium taurocholate, 0.83 mM lecithin, and 45 mM morpholineethansulfonic acid sodium salt (MES, additional buffer component)(Sigma–Aldrich, Bornem, Belgium) in blank FaSSIF. Samples (1 ml) were withdrawn from FaSSIF at 65, 70, 90, 120, 180, and 300 min (i.e., 5, 10, 30, 60, 120, and 240 min after transfer from SGF). All samples were diluted appropriately and analyzed by HPLC-UV.

As a measure of pharmaceutical performance, we used the area under the concentration–time profile during the first 60 min in FaSSIF ($AUC_{60\ min\ FaSSIF}$). The AUC values for the complete profile were not used, given the confounding effect of ITZ nanofiber formation after the 60-min time point (as outlined in Section 3). These AUC values were calculated by linear-trapezoidal integration using the GraphPad Prism software package. We also determined the maximum concentration attained after transfer to FaSSIF ($C_{max\ FaSSIF}$). These *in vitro* parameters were compared against the *in vivo* data.

2.13. HPLC-UV

The chromatographic system consisted of a binary pump (type 1525, Waters, Milford, MA), an autosampler (717 Plus, Waters), and a dual wavelength absorbance detector (type 2487, Waters). A Lichrospher® 100 RP C-18 column (5 μm) (Merck, Darmstadt, Germany) was used for chromatographic separation. The mobile phase consisted of methanol/sodium acetate buffer (25 mM, pH 3.5) 80/20 (v/v%). The flow rate was 1.5 ml/min. The retention time of ITZ under these conditions was 6 min. Calibration curves were linear over a concentration range of 0.01–50 μg/ml. All chromatograms were analyzed using the Breeze software package (Waters).

2.14. In vivo study

All *in vivo* experiments were carried out in accordance with the EC directive 86/609/EEC for animal experiments (license number LA1210261). Approval for this project was granted by the K.U. Leuven Institutional Ethical Committee for Animal Experimentation.

2.14.1. Preparation of formulations

ITZ:SBA-15 1:4 was prepared as described in Section 2.3. An overview of the composition of all formulations evaluated *in vivo* is provided in Table 3. All ITZ:SBA-15:HPMC(AS) formulations were prepared as described in Section 2.10. If required, the amount of formulation to be administered was divided over two capsules, in order to avoid compression of the capsule content. The formulations were filled into hard gelatin capsules (PCcaps size 9) (Capsugel, Bornem, Belgium) by means of a stand, funnel, and tamper (PCcaps kit, Capsugel).

2.14.2. Animals

Male Wistar rats (300–380 g, ca. 9 weeks of age) (Elevage Janvier, Le Genet Saint Isle, France) were used throughout this study. All animals were allowed to acclimatize for at least one week prior to the experiments. Water and feed (58% carbohydrates, 33% proteins, 9% lipids) (ssniff R/M-H, sniff Spezialdiäten, Soest, Germany) were available *ad libitum*.

2.14.3. Dosing

All rats were dosed orally with 1 ± 0.05 mg of ITZ, as either an SBA-15-based formulation, Sporanox® pellets or crystalline drug ($n = 3$). All capsules were administered intragastrically using a dosing syringe plunger (PCcaps kit).

2.14.4. Blood sampling

The multiple blood sampling protocol described here was based on the results of a prior study, demonstrating good reproducibility using a small number of rats [43]. Prior to each blood draw, the rats were warmed in an incubator (37 °C) (Mini-thermacage MK3, Datesand, Manchester, UK) for 15 min to promote bleeding. Subsequently, the animals were placed in a cylindrical restrainer with

adjustable headgate and removable tailgate (Harvard Apparatus, Holliston, MA). Blood samples (500 μl) were taken by individual venipunctures of the lateral tail vein at pre-dose and 1, 2, 3, 5, 7, 9, 12, and 24 h post-dose. Blood was collected into heparin-coated tubes (LH, 68 I.U.) (Vacutainer, Becton Dickinson, Plymouth, UK), and plasma was harvested by centrifugation (3600*g*, 4 °C, 10 min) using an IEC Centra-8R centrifuge (International Equipment Company, Needham Heights, MA). After every blood draw, the rats were released into their cages, where they had free access to feed and water. All plasma samples were stored at −20 °C pending bioanalysis.

2.14.5. Bioanalysis

2.14.5.1. Sample preparation. Hanks' Balanced Salt Solution (800 μl) (Cambrex BioScience, Verviers, Belgium), supplemented with 10 mM of HEPES-buffer (Cambrex), pH adjusted to 7.4 with NaOH (BDH, Poole, England), was added to 200 μl of plasma. This mixture was spiked with 100 μl of internal standard solution [0.5 μM R051012 (Janssen Pharmaceutica) in 0.2 M HCl (VWR International)]. Subsequently, 500 μl of NaOH (2 M) was added to alkalinize the samples. Samples were extracted using 4 ml of diethylether (Lab-Scan, Dublin, Ireland). After centrifugation (3600*g*, 4 °C, 5 min), the upper organic layer was transferred into a test tube and evaporated to dryness. Lastly, the extraction residue was dissolved in 150 μl of a 50/50 (v/v%) methanol/water mixture, transferred into autosampler vials, and analyzed by LC–MS as described below.

2.14.5.2. LC–MS. All plasma samples were quantified for ITZ and OH-ITZ. OH-ITZ is the major active metabolite in humans [32] as well as in rats [44]. Liquid chromatography coupled to mass spectrometry (LC–MS) (Alliance HT system, equipped with a Micromass ZQ 2000 detector; Waters) was used for all bioanalyses. A Novapak C-18 (4 μm) (Waters) column was used. The mobile phase consisted of 84/16 (v/v%) methanol/ammonium acetate buffer (Riedel-de Haën, Seelze, Germany (5 mM, pH 3.3). Samples were run under isocratic conditions (1 ml/min). A post-column flow splitter directed 25% of the flow to the MS, while the remainder was carried to the waste. The mass spectrometer was operated in the positive ion electrospray ionization mode. The voltages at the capillary and cone were tuned to 3.1 kV and 40 V, respectively. The temperatures of the source was set at 120 °C. The desolvation temperature amounted to 350 °C. The gas flow was 500 l/h at the desolvation stage and 50 l/h in the cone. The sodium adducts of ITZ, OH-ITZ, and the internal standard were monitored at *m/z* values of, respectively, 727, 743, and 755. Under the above-mentioned chromatographic conditions, OH-ITZ, ITZ, and the internal standard had retention times of 4.9, 6.9, and 8.4 min, respectively. Integration of the chromatographic peaks was performed using the Empower 2 software package (Waters). The calibration curves for both ITZ and OH-ITZ were linear over the concentration ranges of 7.8–125 nM (low concentration range) and 125–1000 nM (high concentration range). Interday variability for 75 nM (low concentration range) and 750 nM standards (high concentration range) was lower than 10% (RSD) for both analytes ($n = 6$). Recovery of the same standards was within the range of 90–112% ($n = 6$).

2.14.5.3. Data analysis. The observed maximum plasma concentration (C_{max}) and the time of its occurrence (T_{max}) were determined directly from the individual plasma concentration versus time profiles. The area under the plasma concentration versus time curve (AUC) was estimated by trapezoidal integration to the last sampling point (24 h). Whenever the *extent of absorption* is considered in the discussion of the results, it refers to the sum of the AUCs of ITZ and OH-ITZ (AUC_{sum}). Statistical comparison of C_{max} and AUC_{sum} values of the various formulations was performed on the log-transformed data using a one-way analysis of variance (ANOVA) and post hoc Tukey's multiple comparisons test. P values of <0.05 were considered significant. Statistical analysis on the T_{max} values was performed using a Kruskal–Wallis non-parametric test and post hoc Dunn's multiple comparisons test. All statistical analyses were performed in GraphPad Prism for Windows (GraphPad Software, San Diego, CA).

3. Results and discussion

3.1. Nitrogen adsorption

The batch of SBA-15 powder used throughout this study had an average pore diameter of 7.3 nm, a surface area of 862 m^2/g, a pore volume of 1.03 cm^3/g, a micropore volume of 0.09 cm^3/g, and an external surface area of 40 m^2/g.

3.2. Physical characterization of the SBA-15-based formulations: DSC

The DSC-thermograms of crystalline ITZ, glassy ITZ, ITZ:SBA-15 1:4, and ITZ:SBA-15 1:1.5 are depicted in Fig. 2. Crystalline ITZ melts at 165 °C. It is evident from Fig. 2 that the SBA-15-based formulations do not show any signs of crystallinity. Glassy ITZ exhibits a glass transition at 56 °C and features two small endotherms upon heating at 74 °C and 90 °C (inset view Fig. 2). These two thermal events, typical for glassy ITZ, have been ascribed to an increase in rotational mobility (74 °C) followed by the transition of a chiral nematic mesophase to an isotropic liquid (90 °C) [45]. These endotherms enable the unambiguous detection of clusters of glassy ITZ in a formulation. The thermograms of the SBA-15-based formulations do not exhibit these endotherms. The absence of both glassy and crystalline ITZ can be attributed to finite-size effects and thus provides indirect evidence for the effective adsorption of ITZ in the internal pore network of SBA-15. This is in agreement with earlier work, demonstrating that ITZ is indeed confined to the SBA-15 pores upon impregnation with a methylene chloride solution [46].

The thermograms depicted in Fig. 2 were recorded within one week after preparation. Although a physical stability study of the ITZ-loaded SBA-15 was not a part of this study, a prior paper has demonstrated that ITZ confined in SBA-15 remains non-crystalline for at least one year, at 25 °C/52% RH as well as at 25 °C/97% RH [14].

3.3. ITZ supersaturation in SGF and FaSSIF

As mentioned earlier, a prior supersaturation screening had indicated that only HPMC and HPMCAS were capable of providing significant inhibition of ITZ precipitation (in neutral media). Therefore, in this article, only these two polymers were considered for further evaluation. Before discussing the results, it is noteworthy that – at the concentrations applied in these experiments – nor HPMC, HPMCAS, or DMSO (originating from the co-solvent-induced supersaturation) affected the thermodynamic solubility of ITZ. The concentration–time profiles after generation of supersaturation in SGF are depicted in Fig. 3. It appears that, at DS 10 and 20 (i.e., at an initial concentration of 50 and 100 μg/ml), irrespective of the presence of HPMC, no precipitation of ITZ occurred within the time span of the experiment (note that HPMCAS was not tested in SGF because of its insolubility below pH 5.5). It is worth mentioning that, even though the concentrations in solution were monitored only for 120 min, no ITZ precipitation could be observed for at least 8 h (data not shown). Furthermore, concentrations as high as 280 μg/ml (representing a DS of 56) could be obtained without any visually detectable signs of precipitation.

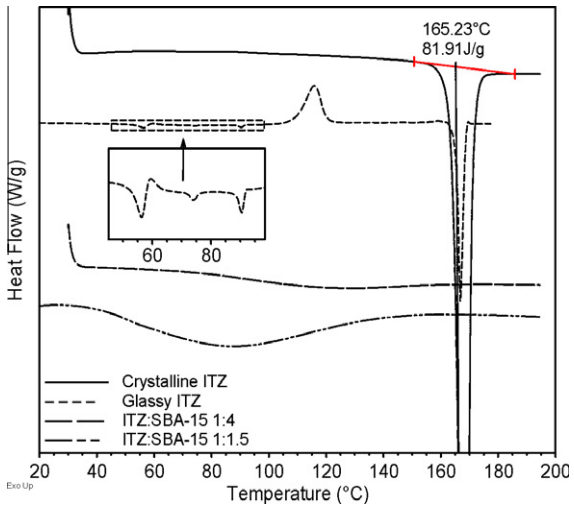

Fig. 2. DSC-thermograms of crystalline ITZ, glassy ITZ, ITZ:SBA-15 1:4 and ITZ:SBA-15 1:1.5. Crystalline ITZ melts at 165 °C. Following the glass transition at 56 °C, two small endotherms appear at 74 and 91 °C (see text for details) in the thermogram of glassy ITZ (inset view). The SBA-15 formulations do not show any signs of crystalline or glassy ITZ.

However, when SBA-15 was predispersed in SGF (0.05% w/v), this affected ITZ supersaturation negatively. Remarkably, rather than initiating a steady decline toward the equilibrium solubility, the presence of SBA-15 caused a quick drop of the supersaturation plateau. It is not unlikely that the presence of a colloidal powder disrupts the stable supersaturation of ITZ. Alternatively, it may well be the case that SBA-15, due to its highly adsorptive character, adsorbs some ITZ on its surface. When both SBA-15 and HPMC were predispersed/predissolved in SGF, the drop in concentration was not as pronounced as in SGF without HPMC, indicating that HPMC can partially compensate for the negative effect of SBA-15 on ITZ supersaturation.

Following generation of supersaturation in FaSSIF, ITZ concentrations declined slowly toward the equilibrium solubility (Fig. 4). When comparing the profiles after generating DS 10 and 20, the concentration profiles only differ during the first 60 min. Afterward, the decrease in concentration was virtually identical for both DS's: 1.3 μg/ml at 60 min, 1.1 μg/ml at 120 min, and 0.7 μg/ml at 240 min. Since the thermodynamic solubility in FaSSIF is 0.3 μg/ml, supersaturation in FaSSIF is maintained for at least four hrs, albeit to a low degree. When HPMC and HPMCAS were predissolved in FaSSIF (0.05% w/v), a significant stabilization of supersaturation was observed, with HPMCAS being clearly superior over HPMC. The mechanisms underlying the stabilizing effect of HPMC and HPMCAS on drug supersaturation have been described elsewhere [27,50–52].

It is important to bear in mind that, although the DS's evaluated in FaSSIF are the same as those in SGF, the absolute concentrations in FaSSIF are about 15-fold lower. Although intuitively one can assume that higher concentrations of precipitation inhibitor would be better suited to stabilize more highly supersaturated solutions, we did not assess this effect in the present study. The rationale for the relatively low stabilizer concentration (0.05% w/v) used throughout this study was twofold. First, our own (unpublished) findings and those of other authors indicate that even very low concentrations of stabilizer (in the same range as the 0.05% used in this study) may be sufficient to effectively inhibit precipitation [27]. Second, 0.05% represents a biopharmaceutically relevant concentration, i.e., a concentration of stabilizer that is likely to be encountered in the *in vivo* situation. The example of Sporanox® may be illustrative. The ITZ:HPMC ratio in Sporanox® is 1:1.5. Complete release of the 100 mg ITZ dose is then accompanied by the dissolution of 150-mg HPMC. Assuming a total intestinal volume of 250 ml, the maximum concentration of HPMC in the gastrointestinal tract would then be 0.6 mg/ml or 0.06% (w/v). Several authors have reported on concentrations of stabilizer as high as 2%. Although such data might provide useful insights into the mechanism underlying supersaturation stabilization, achieving concentrations this high *in vivo* would require a significant increase of the pill burden.

3.4. In vitro release in SGF

The *in vitro* release experiments conducted under sink conditions (SGF + 1% SLS) indicate that more than 85% of ITZ is released from SBA-15 within 10 min (Fig. 5). It is also evident from Fig. 5 that a drug loading of 1:4 and 1:1.5 (ITZ:SBA-15) results in the same release rate. The initial release rate from the commercialized solid dispersion Sporanox® is significantly slower (only 6% after 10 min), yet it also attains 100% release within 120 min. It should be noted that the dissolution of crystalline ITZ was rapid under sink conditions as well, which may be attributed to the affinity of ITZ for the SLS micelles. As a matter of fact, the dissolution of crystalline ITZ was faster than release from Sporanox®, which illustrates that release from Sporanox® is governed by the dissolution of its HPMC matrix.

Under supersaturating conditions (plain SGF), drug release appears to be slower for the SBA-15-based formulations (Fig. 6). After 120 min, ITZ:SBA-15 1:4 and ITZ:SBA-15 1:1.5 reach only 58% and 53% release, respectively, instead of the 100% observed under sink conditions. The release profile of Sporanox® in plain SGF was highly comparable to that recorded in SGF + 1% SLS (Fig. 5). The concentrations resulting from the dissolution of crystalline ITZ could not be detected with our analytical methodology (UV-spectrometry). Obviously, the absence of the solubilizing agent SLS contributes to a slower release from SBA-15. However, decreased

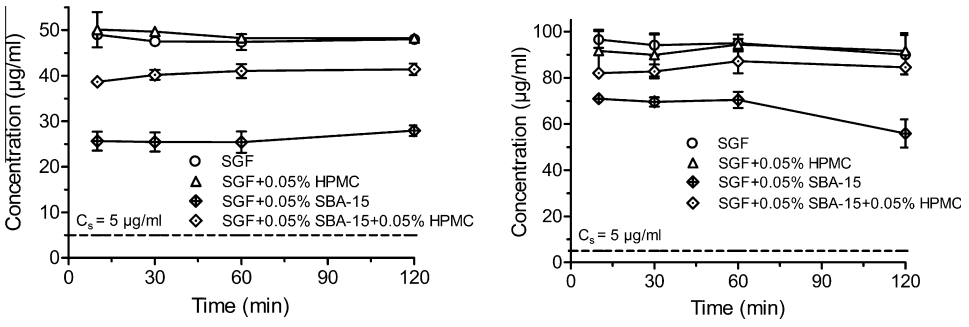

Fig. 3. Supersaturation profiles of ITZ in SGF at DS 10 (left panel) and DS 20 (right panel). The dashed line represents the thermodynamic solubility (C_s) of ITZ in SGF. The (theoretical) initial concentrations at DS 10 and DS 20 were 50 and 100 μg/ml, respectively. When SBA-15 is predispersed in SGF, the supersaturation plateau drops. HPMC can partly compensate for the negative effect of SBA-15 on ITZ supersaturation (seet text for details). Average and standard deviation are depicted (n = 3).

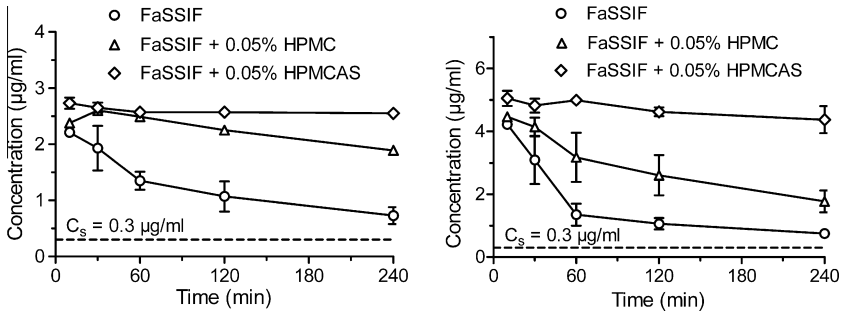

Fig. 4. Supersaturation profiles of ITZ in FaSSIF at DS 10 (left panel) and DS 20 (right panel). The dashed line represents the thermodynamic solubility (C_s) of ITZ in FaSSIF. The (theoretical) initial concentrations at DS 10 and DS 20 were 3 and 6 µg/ml, respectively. Both HPMC and HPMCAS stabilize ITZ supersaturation in FaSSIF, with HPMCAS being superior over HPMC. Average and standard deviation are depicted ($n = 3$).

wettability and/or solubilization constitute only a part of the explanation. As stated above, the SBA-15 carrier itself attenuates ITZ supersaturation, which may explain the lower concentrations observed for the SBA-15-based formulations in plain SGF. The higher plateau for ITZ:SBA-15 1:1.5 when compared to ITZ:SBA-15 1:4 may therefore be attributed to the lower amount of SBA-15 present in the medium. The release profiles that reach only 55% and 77% for ITZ:SBA-15 1:4 and 1:1.5, respectively, may indicate that either a part of the released fraction precipitates or that not all ITZ is released from the silica surface.

Addition of HPMC to ITZ:SBA-15 1:4 enhances the performance of the latter (Fig. 6), which is in agreement with the findings obtained from the supersaturation experiments (Fig. 3). An increase in the amount of HPMC added (from ITZ:SBA-15:HPMC 1:4:1.5 to 1:4:6) resulted only in a minor increase in performance. The relative amount released after 120 min amounted to 69%, 77%, and 81% for ITZ:SBA-15:HPMC 1:4:1.5, ITZ:SBA-15:HPMC 1:4:6, and Sporanox®, respectively.

Although these data, obtained in SGF, clearly illustrate the potential of SBA-15 to enhance ITZ dissolution, the data may not be predictive for the *in vivo* performance. *In vivo*, the increase in pH (and thus, the drop in solubility) when going from the acidic environment of the stomach to the neutral milieu of the small intestine may cause significant precipitation and thus have a dramatic effect on absorption. *In vitro* release experiments simulating this transition are described below.

3.5. In vitro release with pH-shift

In the pH-shift experiments, samples were agitated for 60 min in SGF (maximum concentration in SGF 200 µg/ml), after which 4 ml of SGF was transferred to 36 ml of FaSSIF. As a measure of pharmaceutical performance, we used the area under the concentration–time profile during the first 60 min in FaSSIF ($AUC_{60\ min}$), which proved to be a good predictor of *in vivo* performance (see below). The values of $AUC_{60\ min}$ are provided in Table 2. The maximum concentrations attained in FaSSIF following the pH-shift ($C_{max\ FaSSIF}$) are also given in Table 2.

From Fig. 6, it can be seen that after 60 min in SGF, the release from ITZ:SBA-15 1:4 and Sporanox® amounted to 53% and 68%, respectively. Five minutes after transfer to FaSSIF, the relative amount in solution had dropped to 25% for ITZ:SBA-15 1:4 and to 66% for Sporanox® (Fig. 7). Up to 60 min in FaSSIF, concentrations in solution remain significantly higher for Sporanox® than for ITZ:SBA-15 1:4. Note that 100% in solution in FaSSIF corresponds to an absolute concentration of 20 µg/ml. Thus, any percentage above 1.5% (or 0.3 µg/ml, the thermodynamic solubility of ITZ in FaSSIF) represents a supersaturated state. For all formulations, supersaturation was maintained during the whole time

Table 2
Summary *in vitro* release parameters. Mean values and standard deviation are given ($n = 3$).

Formulation	$C_{max\ FaSSIF}$ (%)[a]	$AUC_{60\ min\ FaSSIF}$ (% min)[b]
Sporanox®	66.3 ± 1.9	2587 ± 136
Crystalline ITZ	5.2 ± 0.1	132 ± 1
ITZ:SBA-15 1:4	25.2 ± 1.1	756 ± 88
ITZ:SBA-15:HPMC 1:4:1.5	35.4 ± 3.3	1180 ± 44
ITZ:SBA-15:HPMC 1:4:6	47.6 ± 2.8	2021 ± 241
ITZ:SBA-15:HPMCAS 1:4:1.5	27.4 ± 0.8	872 ± 42
ITZ:SBA-15:HPMCAS 1:4:6	25.0 ± 1.5	994 ± 30

[a] Maximum release in FaSSIF following transfer from SGF.
[b] Area under the dissolution curve during the first 60 min in FaSSIF.

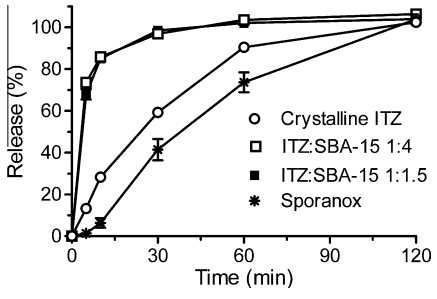

Fig. 5. *In vitro* release profiles recorded under sink conditions (SGF ± 1% SLS). The release profiles for ITZ:SBA-15 1:4 and 1:1.5 are almost identical. ITZ release from SBA-15 occurs much faster than from Sporanox®. All formulations attain 100% release within 120 min. Note that the dissolution of crystalline ITZ was also very rapid under sink conditions, which is due to the high affinity of ITZ for the SLS micelles. Average and standard deviation are depicted ($n = 3$).

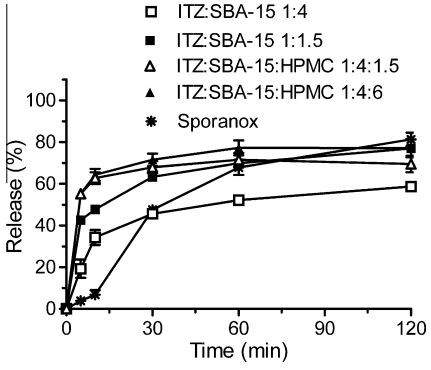

Fig. 6. *In vitro* release profiles recorded under supersaturating conditions (SGF). None of the formulations reaches 100% release within 120 min. The addition of HPMC to ITZ:SBA-15 1:4 enhances its performance. Average and standard deviation are depicted ($n = 3$).

course of the experiment. Crystalline ITZ also generated supersaturation in FaSSIF following transfer from SGF, albeit to a very low degree and only for 120 min.

Remarkably, after 60 min in FaSSIF, ITZ:SBA-15 1:4 exhibits a linear increase in concentration. This peculiar behavior of supersaturated ITZ has been reported earlier [53] and has recently been attributed to the formation of ITZ nanofibers [54]. It has been demonstrated that these nanofibers do not permeate through a Caco-2 cell monolayer, which precludes their intestinal absorption [53]. However, it is unclear whether these nanofibers are also formed *in vivo*. Furthermore, their formation appears inhibited upon addition of a polymer such as HPMC or HPMCAS. It should also be noted that the *in vivo* results of the present study (see below) as well as those obtained in prior work [22], were not indicative for a reduction of absorbability due to ITZ nanofiber formation. For more information regarding the nanofiber formation of ITZ, the reader is referred to Mellaerts et al., 2010 [54].

The better performance of Sporanox® when compared to ITZ:SBA-15 1:4 may be attributed to a combination of several factors. First and foremost, Sporanox® contains HPMC, which is, as demonstrated above, a stabilizer of ITZ supersaturation. After transfer to FaSSIF, the co-dissolved HPMC inhibits ITZ precipitation, whereas uninhibited precipitation takes places of the ITZ molecules that were released from SBA-15. Second, after 60 min in SGF, ITZ release in SGF was higher for Sporanox® than for ITZ:SBA-15 1:4 (68% versus 53%).

In order to enhance its performance, ITZ:SBA-15 1:4 was combined with HPMC and HPMCAS. Fig. 8 illustrates the effect of HPMC (left panel) and HPMCAS (right panel) on the performance of SBA-15. It is evident that the addition of HPMC resulted in higher concentrations in FaSSIF. However, it is remarkable that the *in vitro* performance of ITZ:SBA-15:HPMC 1:4:1.5 remained significantly lower than that of Sporanox®, in spite of the fact that (i) both formulations have the same ITZ:HPMC ratio and (ii) both have a comparable release after 60 min in SGF (71% and 68% for ITZ:SBA-15:HPMC 1:4:1.5 and Sporanox®, respectively). This discrepancy may be explained as follows. After 60 min in SGF, the release profile of Sporanox® is still increasing, whereas the SBA-15-based formulations have reached a plateau (Fig. 6). This suggests that Sporanox® can still release ITZ after transfer to FaSSIF, whereas the SBA-15-based formulations cannot. This may explain the better performance of the former.

As expected, increasing the amount of HPMC (ITZ:SBA-15:HPMC 1:4:6) resulted in an increase in performance. Note that the release after 60 min in SGF is comparable for ITZ:SBA-15:HPMC 1:4:1.5 and ITZ:SBA-15:HPMC 1:4:6 (71% and 77%, respectively). The enhanced ITZ concentrations in FaSSIF for ITZ:SBA-15:HPMC 1:4:6 may therefore be attributed to a more pronounced precipitation inhibition due to the higher HPMC concentrations. Despite the 4-fold higher amount of HPMC, the performance of ITZ:SBA-15:HPMC 1:4:6 remained lower than that of Sporanox®. The explanation for this finding is analogously to that provided in the previous paragraph for ITZ:SBA-15:HPMC 1:4:1.5. Although it seems plausible that the addition of higher amounts of HPMC would have further enhanced the performance of SBA-15, we did not evaluate such a formulation as the drug load would then become unrealistically low.

The addition of HPMCAS resulted only in a marginal increase in the performance of SBA-15 in the pH-shift experiments (Fig. 8, right panel), which is somewhat counterintuitive to its excellent stabilizing effect in FaSSIF. This may be explained in terms of the insolubility of HPMCAS in SGF (the pH-solubility cutoff of the HPMCAS grade used in this study is pH 5.5). When dispersing the ITZ:SBA-15:HPMCAS formulations in SGF, ITZ is released from the SBA-15 pores while HPMCAS remains undissolved. Upon transfer to FaSSIF, the released ITZ molecules are prone to precipitation immediately, since little or no HPMCAS has already gone into solution. The slightly enhanced ITZ concentrations for ITZ:SBA-15:HPMCAS 1:4:6 over ITZ:SBA-15:HPMCAS 1:4:1.5 at the later time points may simply be attributed to the higher concentration of HPMCAS, enabling a more adequate stabilization of supersaturation.

3.6. In vivo study

All formulations that were evaluated in the pH-shift experiments were also evaluated *in vivo*, except for ITZ:SBA-15:HPMCAS 1:4:1.5 since this formulation did not result in an increase in performance when compared to SBA-15 without precipitation inhibitors. Overall, the pharmaceutical performance of all the formulations exhibited the same rank order *in vitro* and *in vivo*,

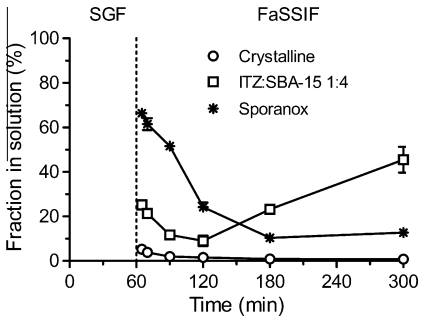

Fig. 7. Concentration–time profiles of ITZ in FaSSIF after transfer from SGF. The enhanced concentrations for Sporanox® when compared to ITZ:SBA-15 1:4 may be attributed to the effect of HPMC. The linear increase in concentration observed for ITZ:SBA-15 1:4 originates from ITZ nanofiber formation (see text for details). Average and standard deviation are depicted ($n = 3$).

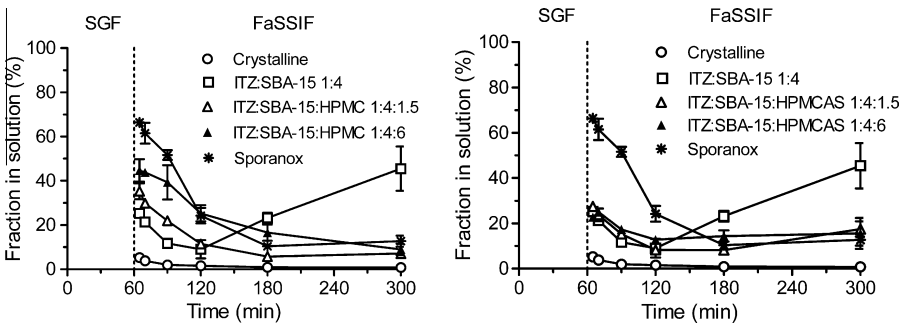

Fig. 8. Concentration–time profiles of ITZ in FaSSIF after transfer from SGF: effect of HPMC (left panel) and HPMCAS (right panel) on the performance of SBA-15. HPMC enhances the performance of SBA-15, whereas HPMCAS does not. Average and standard deviation are depicted ($n = 3$).

the only exception being ITZ:SBA-15:HPMCAS 1:4:6 (see explanation below). A summary of all the formulations that were evaluated *in vivo* and their respective PK parameters is provided in Table 3. From Fig. 9, it is evident that the systemic exposure remained quasi negligible when the rats were dosed with crystalline ITZ. When ITZ was loaded into SBA-15, a significant improvement in rate and extent of absorption was observed. Note that the ITZ pharmacokinetic (PK) profiles are virtually identical for ITZ:SBA-15 1:4 and ITZ:SBA-15 1:1.5, whereas the OH-ITZ plasma concentrations are lower for ITZ:SBA-15 1:1.5. Although this suggests a slightly better performance for ITZ:SBA-15 1:4, there were no statistically significant differences between ITZ:SBA-15 1:4 and ITZ:SBA-15 1:1.5 in terms of AUC_{sum}, C_{max}, or T_{max}. Both ITZ:SBA-15 1:4 and 1:1.5 exhibited significantly lower C_{max} and AUC_{sum} values than Sporanox® (note that the human fraction of dose absorbed of Sporanox® amounts to 85% [49]).

When small amounts of HPMC were added to ITZ:SBA-15 (ITZ:SBA-15:HPMC 1:4:1.5), no significant improvement in terms of rate or extent of absorption was observed when compared to ITZ:SBA-15 1:4 without precipitation inhibitors (Fig. 10). However, ITZ:SBA-15:HPMC 1:4:6 provided a more than 60% increase in extent of absorption when compared to ITZ:SBA-15 1:4 (AUC_{sum} 14,937 ± 1617 versus 8987 ± 2726 nM h). It is noteworthy that, in order to effectively improve *in vivo* performance of SBA-15, relatively high amounts of HPMC were required (ITZ:HPMC ratio 1:6). By contrast, in the commercialized product Sporanox®, an ITZ:HPMC ratio of 1:1.5 is highly effective. Although there was no statistically significant difference in terms of extent of absorption between ITZ:SBA-15:HPMC 1:4:6 (AUC_{sum} 14,937 ± 1617 nM.h) and Sporanox® (AUC_{sum} 17,018 ± 1473 nM.h), Sporanox® did exhibit significantly higher C_{max} values. This is in agreement with the trends observed in the *in vitro* experiments (Fig. 8).

Remarkably, the addition of HPMCAS resulted in a decrease of the performance of SBA-15 (Fig. 10); the plasma concentrations were significantly lower than those observed for ITZ:SBA-15 1:4, and nearly no plasma exposure could be detected prior to the 5-h time point. By contrast, for all of the other SBA-15-based formulations, significant ITZ plasma exposure was detected already 1 h post-dosing. This delay in release was not entirely unexpected, as prior *in vitro* experiments had shown that the disintegration of ITZ:SBA-15:HPMCAS 1:4:6 in SGF was very poor (data not shown), which may be attributed to the insolubility below pH 5.5. The capsule content – although not compressed firmly – did not disperse homogenously in the medium, but rather formed a sticky plug. In neutral media, however, complete disintegration occurred within a few minutes. The repercussion to the *in vivo* situation of this poor disintegration in acidic media is that disintegration (and thus, drug release) probably occurred in the small intestine. If ITZ release is delayed until reaching the small intestine, where (i) the solubility is lower and (ii) supersaturation is much less stable (see Section 3.6), the tendency for precipitation of the released ITZ molecules is much larger than would be the case if ITZ is released in the stomach. A second consequence of the insolubility of HPMCAS at low pH, which is corroborated by the *in vitro* results, is that its (excellent) stabilizing effect on ITZ supersaturation in intestinal media is compromised; if the polymer cannot predissolve in the stomach, it is unable to effectively inhibit precipitation upon entry in the small intestine. It should be pointed out that this latter statement holds true for the approach used in this study, i.e., physically blending the polymer with SBA-15. In HPMCAS-based solid dispersions, where drug release and carrier dissolution occur simultaneously, HPMCAS may still be efficient in stabilizing supersaturation. Although the performance of ITZ:SBA-15:HPMCAS 1:4:6 may have benefited from the addition of a disintegrant, we did not evaluate such a formulation *in vivo*. Even if the capsule content would have dispersed homogenously in the stomach, it is, for the reasons mentioned above, unlikely that HPMCAS would have effectively stabilized ITZ supersaturation.

Table 3
Summary results *in vivo* study ($n = 3$). Average and standard deviation are given for AUC and C_{max} values. Median and range are given for T_{max}.

Formulation	AUC_{ITZ} (nM h)	$C_{max\ ITZ}$ (nM)	$T_{max\ ITZ}$ (h)	$AUC_{OH\text{-}ITZ}$ (nM h)	$C_{max\ OH\text{-}ITZ}$ (nM)	$T_{max\ OH\text{-}ITZ}$ (h)	AUC_{sum} (nM h)	AUC_{sum} relative to Sporanox® (%)
Sporanox®	4168 ± 471	513 ± 130	3 (3–3)	12850 ± 1029	1049 ± 128	5 (3–5)	17018 ± 1473	100
Crystalline ITZ	189 ± 194	15 ± 13	12 (7–12)	511 ± 121	39 ± 12	5 (5–24)	699 ± 109	4
ITZ:SBA-15 1:4	1746 ± 769	197 ± 102	7 (5–7)	7241 ± 1961	606 ± 131	5 (5–7)	8987 ± 2726	53
ITZ:SBA-15 1:1,5	1589 ± 140	202 ± 13	5 (5–5)	4847 ± 644	389 ± 59	5 (5–7)	6436 ± 736	38
ITZ:SBA-15:HPMC 1:4:1,5	2243 ± 817	276 ± 62	5 (3–5)	6433 ± 434	507 ± 68	5 (3–5)	8676 ± 724	51
ITZ:SBA-15:HPMC 1:4:6	3008 ± 598	276 ± 40	5 (5–7)	11929 ± 1100	825 ± 68	5 (5–7)	14,937 ± 1617	88
ITZ:SBA-15:HPMCAS 1:4:6	677 ± 186	83 ± 15	7 (5–7)	2252 ± 916	229 ± 102	5 (5–7)	2928 ± 1102	17

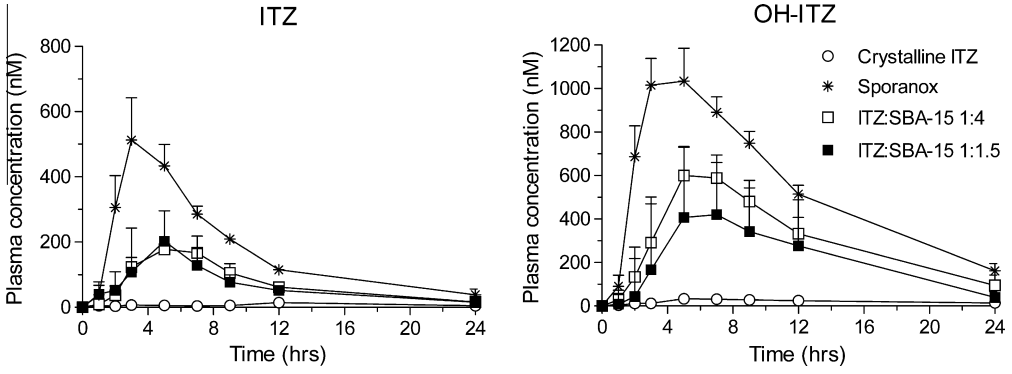

Fig. 9. PK profiles of ITZ (left panel) and OH-ITZ (right panel) for ITZ:SBA-15 1:4, ITZ:SBA-15 1:1.5, crystalline ITZ, and Sporanox®. Loading ITZ in SBA-15 results in a significant improvement of absorption when compared to the crystalline drug. Sporanox® performs better than the SBA-15-based formulations. Average and standard deviation are depicted ($n = 3$).

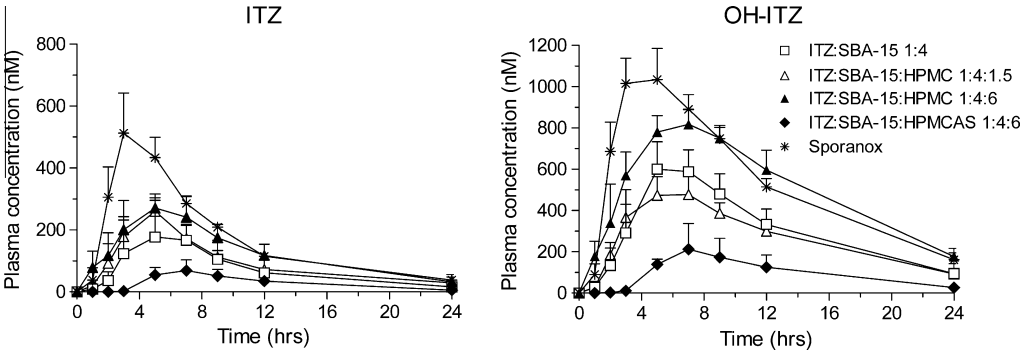

Fig. 10. PK profiles of ITZ (left panel) and OH-ITZ (right panel). When high enough amounts of HPMC (ITZ:SBA-15:HPMC 1:4:6) are added to SBA-15, its *in vivo* performance is effectively enhanced. The addition of HPMCAS affected the performance of SBA-15 negatively (see text for details). Average and standard deviation are depicted ($n = 3$).

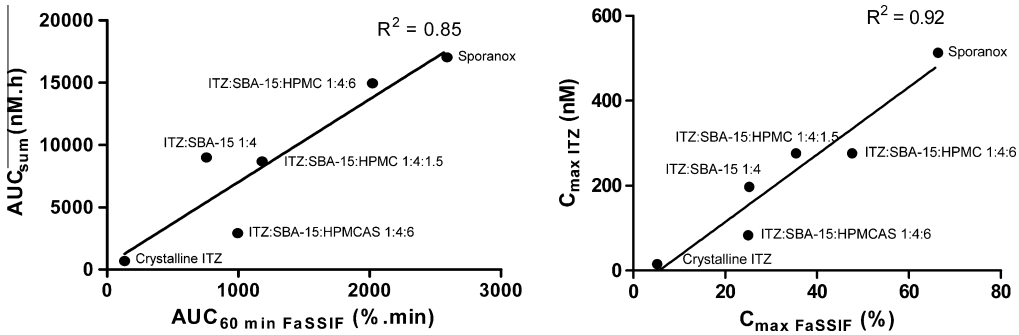

Fig. 11. *In vitro–in vivo* relationship. The *in vivo* performance correlated fairly well with the results obtained in the *in vitro* pH-shift experiments. The *in vivo* performance of ITZ:SBA-15:HPMCAS 1:4:6 was not well predicted by the *in vitro* tests, which is related to its poor disintegration *in vivo* (see text for details).

Although the addition of HPMCAS did not improve the *in vivo* performance of SBA-15, the results do provide us with some useful biopharmaceutical insights. Some authors have suggested that ITZ absorption would benefit from a preferential release in the small intestine [47,48,55]. The rationale behind this statement is that, if ITZ is released primarily in the stomach, precipitation may occur prior to reaching the site of absorption, i.e., the small intestine. By targeting ITZ release to the small intestine, such an effect would be avoided, which would improve absorption. Although the targeting of supersaturating drug delivery systems to the small intestine may well be a useful option for neutral compounds (which usually exhibit higher solubility in intestinal fluids due to solubilization by bile salts and phospholipids) or acidic drugs (which are better soluble at higher pH), our data contradict that this would also hold true for weak bases. Within this study, it was clearly demonstrated that significant ITZ precipitation in the stomach is not very likely to occur. Not only is the thermodynamic solubility of ITZ much higher at low pH, its supersaturation is also very stable in an acidic environment. By contrast, supersaturated ITZ solutions in FaSSIF precipitate rapidly. These findings suggest that the best way to deliver ITZ is to rapidly generate supersaturation in the stomach and then stabilize (e.g., using a polymer such as HPMC) the supersaturated ITZ solution upon entry in the small intestine. The stomach can thus be considered a reservoir, from which supersaturated ITZ is continuously delivered to the small intestine, where absorption can take place. Omitting the gastric dissolution step and releasing the entire ITZ load in the small intestine is not a good approach in our view, as this would lead to a much more pronounced precipitation. The above rationale also suggests that, for poorly soluble weak bases, there is scope for developing mesoporous silica-based gastric retentive dosage forms.

Upon comparison of the *in vitro* and *in vivo* data, it appears that there is a relatively good correlation between $C_{max\ FaSSIF}$ and $C_{max\ ITZ}$ ($R^2 = 0.92$) and between $AUC_{60\ min\ FaSSIF}$ and AUC_{sum} ($R^2 = 0.85$) (Fig. 11). For one formulation, ITZ:SBA-15:HPMCAS 1:4:6, our *in vitro* setup failed to provide a good estimate of *in vivo* performance. This may be attributed to the poor disintegration of this formulation *in vivo* (the consequences of which have been outlined above), an effect which was not accounted for in our *in vitro* setup.

4. Conclusion

In this paper, we evaluated the pharmaceutical performance of formulations consisting of the ordered mesoporous silicate SBA-15 and the precipitation inhibitors HPMC and HPMCAS. Although SBA-15 was found capable of generating ITZ supersaturation in acidic media, its performance was limited due to precipitation of the released ITZ molecules upon entry in the small intestine. The polymer HPMC proved to be a good stabilizer of ITZ supersaturation in intestinal media, and the addition of HPMC to SBA-15 resulted in a more than 60% increase in absorption. HPMCAS, although very efficient in inhibiting ITZ precipitation in intestinal media, was found ineffective *in vivo* due to the fact that it could not predissolve in the stomach.

This study has demonstrated that the approach of combining SBA-15 with an appropriate precipitation inhibitor constitutes a valuable tool to enhance the absorption of poorly soluble weak bases such as ITZ.

Acknowledgments

This study was supported by grants from the Industrial Research Fund (IOF) and the "Onderzoeksfonds" of the K.U. Leuven.

MVS acknowledges the Institute for the Promotion of Innovation through Science and Technology in Flanders (IWT Vlaanderen) for a PhD grant. Randy Mellaerts is a postdoctoral researcher of the Research Foundation – Flanders (FWO Vlaanderen). Professor Jos Hoogmartens of the Laboratory for Pharmaceutical Analysis of the K.U. Leuven is acknowledged for carrying out the head-space chromatography experiments. The help of Loes Verheyden during the nitrogen adsorption experiments was greatly appreciated.

References

[1] C.A. Lipinski, F. Lombardo, B.W. Dominy, P.J. Feeney, Experimental and computational approaches to estimate solubility and permeability in drug discovery and development settings, Adv. Drug Deliv. Rev. 46 (2001) 3–26.
[2] C.A. Lipinski, Drug-like properties and the causes of poor solubility and poor permeability, J. Pharmacol. Toxicol. Methods 44 (2000) 235–249.
[3] P. Gribbon, A. Sewing, High-throughput drug discovery: what can we expect from HTS, Drug Discov. Today 10 (2005) 17–22.
[4] B.C. Hancock, G. Zografi, Characteristics and significance of the amorphous state in pharmaceutical systems, J. Pharm. Sci. 86 (1997) 1–12.
[5] C. Leuner, J. Dressman, Improving drug solubility for oral delivery using solid dispersions, Eur. J. Pharm. Biopharm. 50 (2000) 47–60.
[6] D.Q.M. Craig, The mechanisms of drug release from solid dispersions in water-soluble polymers, Int. J. Pharm. 231 (2002) 131–144.
[7] A.T. Serajuddin, Solid dispersion of poorly water-soluble drugs: early promises, subsequent problems, and recent breakthroughs, J. Pharm. Sci. 88 (1999) 1058–1066.
[8] H. Van Damme, Nanoscale and mesoscale morphology of silica surfaces, in: E. Papirer (Ed.), Adsorption on Silica Surfaces, Marcel Dekker Inc., New York, 2000, pp. 119–165.
[9] G. Dosseh, Y. Xia, C. Alba-Simionesco, Cyclohexane and benzene confined in MCM-41 and SBA-15: confinement effects on freezing and melting, J. Phys. Chem. 107 (2003) 6445–6453.
[10] D. Morineau, Y. Xia, C. Alba-Simionesco, Finite-size and surface effects on the glass transition of liquid toluene confined in cylindrical mesopores, J. Chem. Phys. 117 (2002) 8966–8972.
[11] K. Morishige, K. Kawano, Freezing and melting of methanol in a single cylindrical pore: dynamical supercooling and vitrification of methanol, J. Chem. Phys. 112 (2000) 11023.
[12] M. Van Speybroeck, V. Barillaro, T.D. Thi, R. Mellaerts, J. Martens, J. Van Humbeeck, J. Vermant, P. Annaert, G. Van den Mooter, P. Augustijns, Ordered mesoporous silica material SBA-15: a broad-spectrum formulation platform for poorly soluble drugs, J. Pharm. Sci. 98 (2009) 2648–2658.
[13] S. Shen, W.K. Ng, L. Chia, Y. Dong, R.B.H. Tan, Stabilized amorphous state of ibuprofen by co-spray drying with mesoporous SBA-15 to enhance dissolution properties, J. Pharm. Sci. (2009).
[14] R. Mellaerts, K. Houthoofd, K. Elen, H. Chen, M. Van Speybroeck, J. Van Humbeeck, P. Augustijns, J. Mullens, G. Van den Mooter, J.A. Martens, Aging behavior of pharmaceutical formulations of itraconazole on SBA-15 ordered mesoporous silica carrier material, Micropor. Mesopor. Mater. 130 (2010) 154–161.
[15] F. Qu, G. Zhu, S. Huang, S. Li, J. Sun, D. Zhang, S. Qiu, Controlled release of Captopril by regulating the pore size and morphology of ordered mesoporous silica, Micropor. Mesopor. Mater. 92 (2006) 1–9.
[16] R. Mellaerts, C.A. Aerts, J. Van Humbeeck, P. Augustijns, G. Van den Mooter, J.A. Martens, Enhanced release of itraconazole from ordered mesoporous SBA-15 silica materials, Chem. Commun. (2007) 1375–1377.
[17] I. Izquierdo-Barba, A. Martinez, A.L. Doadrio, J. Pérez-Pariente, M. Vallet-Regí, Release evaluation of drugs from ordered three-dimensional silica structures, Eur. J. Pharm. Sci. 26 (2005) 365–373.
[18] J. Andersson, J. Rosenholm, S. Areva, M. Lindén, Influences of material characteristics on ibuprofen drug loading and release profiles from ordered micro- and mesoporous silica matrices, Chem. Mater. 16 (2004) 4160–4167.
[19] D. Zhao, J. Feng, Q. Huo, N. Melosh, G. Fredrickson, B. Chmelka, G. Stucky, Triblock copolymer syntheses of mesoporous silica with periodic 50–300 angstrom pores, Science 279 (1998) 548–552.
[20] C.T. Kresge, M.E. Leonowicz, W.J. Roth, J.C. Vartuli, J.S. Beck, Ordered mesoporous molecular sieves synthesized by a liquid-crystal template mechanism, Nature 359 (1992) 710–712.
[21] S. Inagaki, A. Koiwai, N. Suzuki, Y. Fukushima, K. Kuroda, Syntheses of highly ordered mesoporous materials, FSM-16, derived from Kanemite, Bullet. Chem. Soc. Jpn. 69 (1996) 1449–1457.
[22] R. Mellaerts, R. Mols, J.A.G. Jammaer, C.A. Aerts, P. Annaert, J. Van Humbeeck, G. Van den Mooter, P. Augustijns, J.A. Martens, Increasing the oral bioavailability of the poorly water soluble drug itraconazole with ordered mesoporous silica, Eur. J. Pharm. Biopharm. 69 (2008) 223–230.
[23] J. Brouwers, M.E. Brewster, P. Augustijns, Supersaturating drug delivery systems: the answer to solubility-limited oral bioavailability, J. Pharm. Sci. 98 (2009) 2549–2572.
[24] H.R. Guzmán, M. Tawa, Z. Zhang, P. Ratanabanangkoon, P. Shaw, C.R. Gardner, H. Chen, J. Moreau, O. Almarsson, J.F. Remenar, Combined use of crystalline salt forms and precipitation inhibitors to improve oral absorption of celecoxib from solid oral formulations, J. Pharm. Sci. 96 (2007) 2686–2702.
[25] P. Gao, B.D. Rush, W.P. Pfund, T. Huang, J.M. Bauer, W. Morozowich, M. Kuo, M.J. Hageman, Development of a supersaturable SEDDS (S-SEDDS) formulation of paclitaxel with improved oral bioavailability, J. Pharm. Sci. 92 (2003) 2386–2398.
[26] P. Gao, M.E. Guyton, T. Huang, J.M. Bauer, K.J. Stefanski, Q. Lu, Enhanced oral bioavailability of a poorly water soluble drug PNU-91325 by supersaturatable formulations, Drug Dev. Ind. Pharm. 30 (2004) 221–229.
[27] P. Gao, A. Akrami, F. Alvarez, J. Hu, L. Li, C. Ma, S. Surapaneni, Characterization and optimization of AMG 517 supersaturatable self-emulsifying drug delivery system (S-SEDDS) for improved oral absorption, J. Pharm. Sci. 98 (2009) 516–528.
[28] T. Heikkilä, J. Salonen, J. Tuura, N. Kumar, T. Salmi, D.Y. Murzin, M.S. Hamdy, G. Mul, L. Laitinen, A.M. Kaukonen, J. Hirvonen, V. Lehto, Evaluation of mesoporous TCPSi, MCM-41, SBA-15, and TUD-1 materials as API carriers for oral drug delivery, Drug Deliv. 14 (2007) 337–347.
[29] G.L. Amidon, H. Lennernäs, V.P. Shah, J.R. Crison, A theoretical basis for a biopharmaceutic drug classification: the correlation of in vitro drug product dissolution and in vivo bioavailability, Pharm Res 12 (1995) 413–420.
[30] J. Peeters, P. Neeskens, J.P. Tollenaere, P. Van Remoortere, M.E. Brewster, Characterization of the interaction of 2-hydroxypropyl-beta-cyclodextrin with itraconazole at pH 2, 4, and 7, J. Pharm. Sci. 91 (2002) 1414–1422.
[31] A.G. Prentice, A. Glasmacher, Making sense of itraconazole pharmacokinetics, J. Antimicrob. Chemother. 56 (Suppl. 1) (2005) i17–i22.
[32] J. Heykants, A. Van Peer, V. Van de Velde, P. Van Rooy, W. Meuldermans, K. Lavrijsen, R. Woestenborghs, J. Van Cutsem, G. Cauwenbergh, The clinical pharmacokinetics of itraconazole: an overview, Mycoses 32 (Suppl. 1) (1989) 67–87.
[33] T.C. Hardin, J.R. Graybill, R. Fetchick, R. Woestenborghs, M.G. Rinaldi, J.G. Kuhn, Pharmacokinetics of itraconazole following oral administration to normal volunteers, Antimicrob. Agents Chemother. 32 (1988) 1310–1313.
[34] D. Lange, J.H. Pavao, J. Wu, M. Klausner, Effect of a cola beverage on the bioavailability of itraconazole in the presence of H2 blockers, J. Clin. Pharmacol. 37 (1997) 535–540.
[35] S. Jaruratanasirikul, A. Kleepkaew, Influence of an acidic beverage (Coca-Cola) on the absorption of itraconazole, Eur. J. Clin. Pharmacol. 52 (1997) 235–237.
[36] A. Stein, T. Daneshmend, D. Warnock, N. Bhaskar, J. Burke, C. Hawkey, The effects of H2-receptor antagonists on the pharmacokinetics of itraconazole, a new oral antifungal, Br. J. Clin. Pharmacol. 27 (1989) 105–106.
[37] A. Galarneau, M. Nader, F. Guenneau, F. DiRenzo, A. Gedeon, Understanding the stability in water of mesoporous SBA-15 and MCM-41, J. Phys. Chem. 111 (2007) 8268–8277.
[38] S. Brunauer, P.H. Emmett, E. Teller, Adsorption of gases in multimolecular layers, J. Am. Chem. Soc. 60 (1938) 309–319.
[39] B.C. Lippens, J.H. De Boer, Studies on pore systems in catalysts. V. The *t*-method, J. Catal. 4 (1965) 319–323.
[40] E.P. Barrett, L.G. Joyner, P.P. Halenda, The determination of pore volume and area distribution in porous substances, J. Am. Chem. Soc. 73 (1951) 373–380.
[41] S. Janssens, H.N. de Armas, C.J. Roberts, G. Van den Mooter, Characterization of ternary solid dispersions of itraconazole, PEG 6000, and HPMC 2910 E5, J. Pharm. Sci. 97 (2008) 2110–2120.
[42] M. Vertzoni, N. Fotaki, E. Kostewicz, E. Stippler, C. Leuner, E. Nicolaides, J. Dressman, C. Reppas, Dissolution media simulating the intralumenal composition of the small intestine: physiological issues and practical aspects, J. Pharm. Pharmacol. 56 (2004) 453–462.
[43] C. Mackie, K. Wuyts, M. Haseldonckx, S. Blokland, P. Gysemberg, I. Verhoeven, P. Timmerman, M. Nijsen, New model for intravenous drug administration and blood sampling in the awake rat, designed to increase quality and throughput for in vivo pharmacokinetic analysis, J. Pharmacol. Toxicol. Methods 52 (2005) 293–301.
[44] S.D. Yoo, S.H. Lee, E. Kang, H. Jun, J.Y. Jung, J.W. Park, K.H. Lee, Bioavailability of itraconazole in rats and rabbits after administration of tablets containing solid dispersion particles, Drug Dev. Ind. Pharm. 26 (2000) 27–34.
[45] K. Six, G. Verreck, J. Peeters, K. Binnemans, H. Berghmans, P. Augustijns, R. Kinget, G. Van den Mooter, Investigation of thermal properties of glassy itraconazole: identification of a monotropic mesophase, Thermochim. Acta 376 (2001) 175–181.
[46] R. Mellaerts, J.A.G. Jammaer, M. Van Speybroeck, H. Chen, J. Van Humbeeck, P. Augustijns, G. Van den Mooter, J.A. Martens, Physical state of poorly water soluble therapeutic molecules loaded into SBA-15 ordered mesoporous silica carriers: a case study with itraconazole and ibuprofen, Langmuir 24 (2008) 8651–8659.
[47] D.A. Miller, J.C. DiNunzio, W. Yang, J.W. McGinity, R.O.3. Williams, Enhanced in vivo absorption of itraconazole via stabilization of supersaturation following acidic-to-neutral pH transition, Drug Dev. Ind. Pharm. 34 (2008) 890–902.
[48] J.C. Dinunzio, D.A. Miller, W. Yang, J.W. McGinity, R.O.3. Williams, Amorphous compositions using concentration enhancing polymers for improved bioavailability of itraconazole, Mol. Pharmacol. 5 (2008) 968–980.
[49] M.E. Brewster, G. Verreck, I. Chun, J. Rosenblatt, J. Mensch, A. Van Dijck, M. Noppe, A. Ariën, M. Bruining, J. Peeters, The use of polymer-based electrospun nanofibers containing amorphous drug dispersions for the delivery of poorly water-soluble pharmaceuticals, Pharmazie 59 (2004) 387–391.
[50] D.T. Friesen, R. Shanker, M. Crew, D.T. Smithey, W.J. Curatolo, J.A.S. Nightingale, Hydroxypropyl methylcellulose acetate succinate-based spray-dried dispersions: an overview, Mol. Pharmacol. 5 (2008) 1003–1019.

[51] K.H. Ziller, H. Rupprecht, Control of crystal growth in drug suspensions: 1. Design of a control unit and application to acetaminophen suspensions, Drug Dev. Ind. Pharm. 14 (1988) 2341–2370.
[52] S.L. Raghavan, A. Trividic, A.F. Davis, J. Hadgraft, Crystallization of hydrocortisone acetate: influence of polymers, Int. J. Pharm. 212 (2001) 213–221.
[53] R. Mellaerts, R. Mols, P. Kayaert, P. Annaert, J. Van Humbeeck, G. Van den Mooter, J.A. Martens, P. Augustijns, Ordered mesoporous silica induces pH-independent supersaturation of the basic low solubility compound itraconazole resulting in enhanced transepithelial transport, Int. J. Pharm. 357 (2008) 169–179.
[54] R. Mellaerts, A. Aerts, T. P. Caremans, J. Vermant, G. Van den Mooter, J. A. Martens, P. Augustijns, Growth of itraconazole nanofibers in supersaturated simulated intestinal fluid, Mol. Pharmacol., in press, doi:10.1021/mp900300j.
[55] D.A. Miller, J.C. DiNunzio, W. Yang, J.W. McGinity, R.O.3. Williams, Targeted intestinal delivery of supersaturated itraconazole for improved oral absorption, Pharm. Res. 25 (2008) 1450–1459.